Journal of Nuclear Materials 382 (2008) 190–196

Contents lists available at ScienceDirect

Journal of Nuclear Materials

journal homepage: www.elsevier.com/locate/jnucmat

Cluster-dynamics modelling of defects in α-iron under cascade damage conditions

E. Meslin [a,*], A. Barbu [a], L. Boulanger [a], B. Radiguet [b], P. Pareige [b], K. Arakawa [c], C.C. Fu [a]

[a] Service de Recherches de Métallurgie Physique, CEA/Saclay, 91191 Gif-sur-Yvette cedex, France
[b] Groupe de Physique des Matériaux UMR-CNRS 6634, Equipe de Recherche Technologique, No. 1000, Université de Rouen, B.P. 12, 76801 Saint Etienne du Rouvray, France
[c] Research Center for Ultra-High Voltage Electron Microscopy, Osaka University, 7-1, Mihogaoka, Ibaraki, Osaka 567-0047, Japan

ARTICLE INFO

PACS:
61.82.Bg
61.72.Ff
61.72.Ji

ABSTRACT

We report the calibration of a rate theory numerical code capable to reproduce the agglomeration of point-defects produced in α-iron by irradiation under cascade damage conditions. The input parameters are obtained by performing transmission electron microscopy (TEM) experiments in α-iron. It was irradiated at temperatures between 200 and 400 °C with high flux krypton ion under resolvable point-defect cluster conditions. The TEM analyse of the sample irradiated at the highest temperature reveals the presence of two dislocation loop populations: large ones are decorated with small ones, both vacancy and interstitial in type. The vacancy loops are proposal to be located in the compressive side of the large interstitial loops.

1. Introduction

The neutron irradiation of reactor pressure vessel (RPV) steels causes the increase of the ductile–brittle transition temperature. This mechanical properties degradation is partly due to the formation of nanometer-size solute and point-defect (PD) clusters. Therefore, it is a crucial issue to understand their formation. In high copper content RPV steels, it is generally admitted that a homogeneous precipitation mechanism is at the origin of the experimentally observed copper-enriched clusters [1,2]. However, it has been recently shown that this mechanism cannot explain the formation of such clusters in low copper content FeCu model alloys [3,4]. This conclusion was obtained by irradiating a FeCu-0.1 wt% binary alloy with energetic electrons and ions. The geometry of the samples and the damage rate were chosen to give approximately the same supersaturation of isolated point-defects in both conditions. At variance with ion irradiation, no copper cluster was detected by 3D atom probe (3DAP) after electron irradiation, where only isolated Frenkel pairs are created. The main difference between both kinds of irradiation is the formation of small PD clusters in the core of displacement cascades under ion irradiation, as predicted by results of molecular dynamics (MD) simulations in α-iron [5]. We therefore suggested that the formation of copper rich clusters under cascade damage conditions occurs via a heterogeneous precipitation on PD clusters. Calculations carried out with a rate theory (RT) code, taking simultaneously into account the clustering of point-defects and the formation of copper precipitates, assuming a homogeneous precipitation mechanism [6], confirmed this assumption. Indeed, no significant copper precipitation under cascade conditions was obtained. The PD clusters were modelized by using a code calibrated on transmission electron microscopy (TEM) analyse of ferritic alloys irradiated with 1 MeV electron at high damage rates [7]. This calibration was the beginning of a complete study devoted to the modelling of the irradiation induced damage in α-iron. The first part treated the simple case of electron irradiation and assumed the PD clusters to be immobile, independent of their size. To go further, a more extensive study is carried out within the PERFECT European project [8]. Ferritic model alloys were irradiated with neutrons in the BR2 Belgium test reactor and the resulting damage was characterized by complementary experimental techniques such as 3DAP or TEM. PD clusters larger than about 2 nm are visible by TEM as dislocation loop or cavity, but since the clusters formed under neutron irradiation are small, an important part of the size distribution cannot be given by experiments. They can only be investigated by modelling. For this reason, we undertook the experimental calibration of our rate theory model under cascade conditions by using simple ion irradiated α-iron. To ensure the validity of the calibration, it must be carried out within a large temperature range and account for the mobility of small PD clusters, predicted by previous MD simulations [9] and recent *ab initio* calculations [10,11]. The purpose of this paper is precisely to report the experimental study of the PD clusters induced and to describe the calibration of the rate theory model under cascade damage irradiation.

* Corresponding author. Tel.: +33 1 69082168; fax: +33 1 69086667.
E-mail address: estelle.meslin@cea.fr (E. Meslin).

0022-3115/$ - see front matter
doi:10.1016/j.jnucmat.2008.08.010

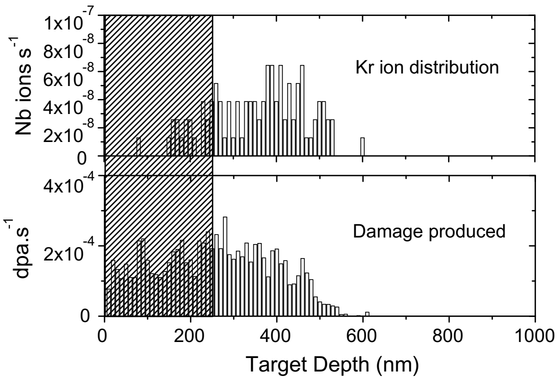

Fig. 1. Damage induced by 1.5 MeV Kr ions in an iron target (SRIM calculation [13]). An energy threshold of 40 eV for the iron atom displacement was chosen. The number of implanted ions per second and the dose rate at each thickness were calculated using an ion flux of 1.1×10^{11} ions cm^{-2} s^{-1}. The dashed area in the figure corresponds to the range of thicknesses visible by TEM, where the damage is likely homogeneous.

2. Experimental study

2.1. Experimental set-up

This study was performed on a pure iron sample provided by the Ecole des Mines of Saint-Etienne. It contains less than 5 wt ppm of carbon and nitrogen and less than 10 wt ppm of silicon. Other elements are less than 1 wt ppm. For TEM investigations, 3 mm disc samples were jet electropolished with a Struers Tenupol 2 device using a solution of 10% perchloric acid and 20% butoxy-ethanol-2 in ethanol at −40 °C until perforation. With this preparation method, we cannot avoid a slight surface oxidation, which introduces a granite-like contrast on the thin foil. The minimal resolvable size of PD clusters was thus 2 nm. The TEM thin foils were then irradiated in the Van de Graaff accelerator ARTHUR of SRMP/CEA at three temperatures (200, 300 and 400 °C) with 1.5 MeV Kr ions. At this energy, the mean projected range of ions is about 350 nm. Since the relevant thickness of the area observable by TEM is around 100 nm, very few atoms were implanted. Most of them passed through the samples and the damage produced is quite homogeneous in the thin foil (Fig. 1). To be consistent with the previous calibration of the model [7], carried out using 1 MeV electron irradiation, the ion flux was chosen to obtain the same damage rate: 1.5×10^{-4} dpaNRT s^{-1}. It was calculated within the simplified NRT approach [12] with the SRIM code [13]. We obtained an ion flux equal to 1.1×10^{11} ions cm^{-2} s^{-1}. We checked that under these conditions, the sputtering rate is very low, equal to 1.7×10^{-7} ion s^{-1}. The irradiation doses were optimized to obtain a damage quantitatively analysable by TEM. The alloys were thus irradiated at 200 °C up to 1.2 dpaNRT, 300 °C up to 0.48 dpaNRT and 400 °C up to 0.2 and 0.5 dpaNRT.

After irradiation, classical TEM observations were performed in a Philips CM20 electron microscope to determine the number density, the size distribution and the nature of dislocation loops. To avoid a possible effect of grain orientation due to the surface image force acting on the loops [14], the number densities were always calculated in {100} orientated grains. These densities were obtained by plotting the projected number density Δp as a function of sample thickness. For this purpose, two images under different diffracting conditions were performed (Fig. 2). The first one is in two-beams dynamical conditions to measure the thickness using similar thickness fringes and the second one is in kinematical conditions to obtain a better contrast of dislocation loops. The number density of dislocation loops is $\Delta L = \Delta p/(e - 2 \cdot Z_d)$, where e and Z_d are the thicknesses of the thin foil and of the denuded zone near the surface, respectively.

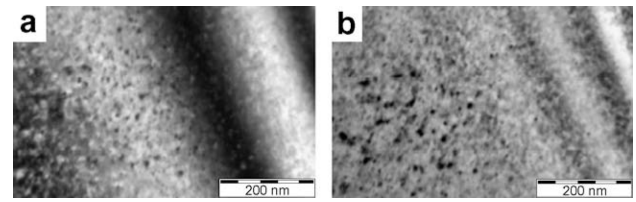

Fig. 2. Determination of the loop number density. The thickness of the specimen at each point is first obtained by using similar thickness fringes (a) in dynamical conditions and the number of loops in each area is calculated (b) in kinematical conditions. See text for more details.

Several techniques can be used to determine the nature of dislocation loops, depending on their size [15]. The loops with a diameter larger than 10 nm were investigated by the classical method of external/internal contrast [16]. For the smaller ones, as the direct methods of black/white analysis or 2 1/2D technique, based on stereomicroscopy, are difficult to apply and have been shown to be inefficient, e.g. in copper [17], we used an indirect determination based on the bias dependence of dislocation loops, already used in α-iron [18]. The bias factor of dislocation loops for self-interstitial atoms (SIA) is larger than for vacancies (V), independent of the loop nature. This difference leads to a net flux of SIA toward loops of both nature. Then, interstitial loops grow whereas vacancy ones shrink during electron irradiation. This is the reason why we performed 2-MeV electron irradiation on the Kr ion irradiated sample in the HVEM Hitachi 3000 of the University of Osaka.

2.2. Results

TEM observations show that when the temperature increases from 200 to 400 °C, the trends of loops number density is to decrease when their size increases (Table 1 and Fig. 3). Also, the width of the distribution increases with temperature (black distribution in the Fig. 4).

After irradiation at 400 °C and 0.5 dpaNRT, the loops are large enough so their Burgers vector and nature can be easily analysed. Fig. 5 shows that two loop populations are present: one is located randomly in the thin foil and has a mean diameter of 20 nm and the other is in the vicinity of the first one, with a smaller mean diameter of 8 nm. We noticed that the most appropriate imaging conditions to see the two loop populations are obtained when the grains are orientated close to a $\langle 110\rangle$ zone axis, as for the Fig. 5 and the Fig. 6(e). The former has a poor quality because it was obtained while the specimen was tilted over a large angle. We can yet distinguish small loops. The Burgers vector analyse of the larger loops revealed that most of them are $\langle 100\rangle$ loops (Fig. 6), but a few $1/2\langle 111\rangle$ ones were also observed. This atypical character of iron compared with other bcc metals, where the dislo-

Table 1
Number density (ΔL) and mean diameter ($\bar{d}$) of loops formed in the studied material irradiated at different temperatures

T	Dose		ΔL	$\bar{d}$
(°C)	(ions cm^{-2})	(dpaNRT)	(cm^{-3})	(nm)
200	8.7 10^{14}	1.2	>10^{16}	10 ±4
300	3.5 10^{14}	0.48	3 ±1 10^{15}	15 ±7
400	1.4 10^{14}	0.20	2 ±0.5 10^{15}	18 ±9

Doses in ions cm^{-2} were calculated by measuring the ion beam current each 7 min using Faraday cages. Doses in dpaNRT were obtained with the SRIM code [13]. The indicated error bar on the mean loop diameter $\bar{d}$ is the statistical standard deviation.